JACS Au
AN OPEN ACCESS JOURNAL OF THE AMERICAN CHEMICAL SOCIETY

pubs.acs.org/jacsau
Article

Light-Induced Reactivity Switch at O_2−Activating Bioinspired Copper(I) Complexes

Donglin Diao,[‖] Anna Baidiuk,[‖] Leo Chaussy, Iago De Assis Modenez, Xavi Ribas, Marius Réglier, Vlad Martin-Diaconescu, Paola Nava,* A. Jalila Simaan,* Alexandre Martinez,* and Cédric Colomban*

Cite This: *JACS Au* 2024, 4, 1966−1974
Read Online

ACCESS | Metrics & More | Article Recommendations | Supporting Information

ABSTRACT: Using light to unveil unexplored reactivities of earth-abundant metal−oxygen intermediates is a formidable challenge, given the already remarkable oxidation ability of these species in the ground state. However, the light-induced reactivity of Cu−O_2 intermediates still remains unexplored, due to the photoejection of O_2 under irradiation. Herein, we describe a photoinduced reactivity switch of bioinspired O_2-activating Cu^I complexes, based on the archetypal tris(2-pyridyl-methyl)amine (**TPA**) ligand. This report represents a key precedent for light-induced reactivity switch in Cu−O_2 chemistry, obtained by positioning C−H substrates in close proximity of the active site. Open and caged Cu^I complexes displaying an internal aryl ether substrate were evaluated. Under light, a Cu−O_2 mediated reaction takes place that induces a selective conversion of the internal aryl ether unit to a phenolate-CH_2− moiety with excellent yields. This light-induced transformation displays high selectivity and allows easy postfunctionalization of **TPA**-based ligands for straightforward preparation of challenging heteroleptic structures. In the absence of light, O_2 activation results in the standard oxidative cleavage of the covalently attached substrate. A reaction mechanism that supports a monomeric cupric-superoxide-dependent reactivity promoted by light is proposed on the basis of reactivity studies combined with (TD-) DFT calculations.

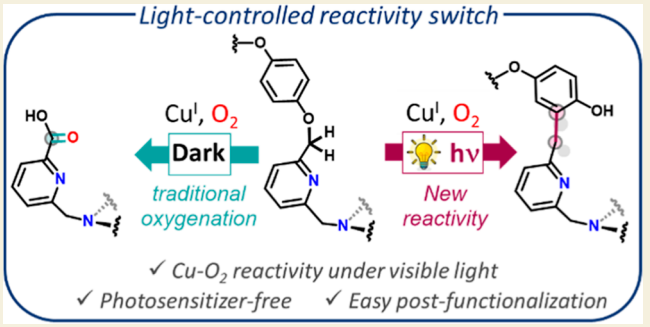

KEYWORDS: *dioxygen activation, photochemistry, reactivity switch, copper, bioinorganic chemistry*

INTRODUCTION

Molecular oxygen (O_2) can be considered the ultimate "green" oxidant. In nature, O_2 activation at metalloproteins enables the most challenging reactions (eg oxidation of methane) through the formation of powerful metal-oxo oxidants.[1] Mononuclear Cu^{II}-superoxo species, which are the initial intermediates produced at several O_2-activating copper enzymes, have attracted considerable attention due to their hydrogen-atom-abstracting capability (HAA) on substrates.[2−6] Exploring O_2 activation pathways on low-molecular-weight models has allowed to gain fundamental knowledge on the ground state reactivity of Cu−O_2 species.[7−13]

The use of visible light in photocatalytic processes is another key aspect of green technologies that has become, in recent years, a powerful tool for developing synthetic transformations under mild conditions. However, the vast majority of photocatalysts are based on precious, heavy transition-metal [ruthenium(II), iridium(III), osmium(II), rhenium(I)].[14−18] Therefore, proposing new photocatalysts based on earth-abundant and biocompatible 3d-metals is of crucial interest.[19] Using light to unveil unexplored reactivities of earth-abundant metal−oxygen intermediates is a formidable challenge, given the already remarkable oxidation ability of these species in the ground state.[20,21] Bridging the chemistry of bioinspired O_2 activating complexes with photocatalysis offers exciting opportunities to environmentally friendly, low-cost, and safe chemical processes. In particular, the discovery of new light-induced reactivities of Cu−O_2 species, which cannot be accessed in their ground state, is of particular interest given the abundance of copper in enzymatic active sites and their often not fully elucidated mechanism of action. However, little is currently known about this emerging field that could, potentially, expand the repertoire of reactions catalyzed under mild conditions.[22] Studying Cu−O_2 reactivity under light remains a challenge due to O_2 photoejection.[23] It was indeed observed that low temperature photoexcitation of mononuclear Cu^{II}-superoxide complexes based on the tris(2-pyridylmethyl)amine (**TPA**) or tris(2-aminoethyl)amine (**TREN**) ligands, results in a reversible copper−oxygen bond

Received: February 28, 2024
Revised: March 28, 2024
Accepted: March 29, 2024
Published: April 29, 2024

cleavage, releasing dioxygen (Figure 1). The photorelease of O_2, via an one-photon two-electron mechanism, was also observed with dinuclear Cu^{II}-peroxo species.[21]

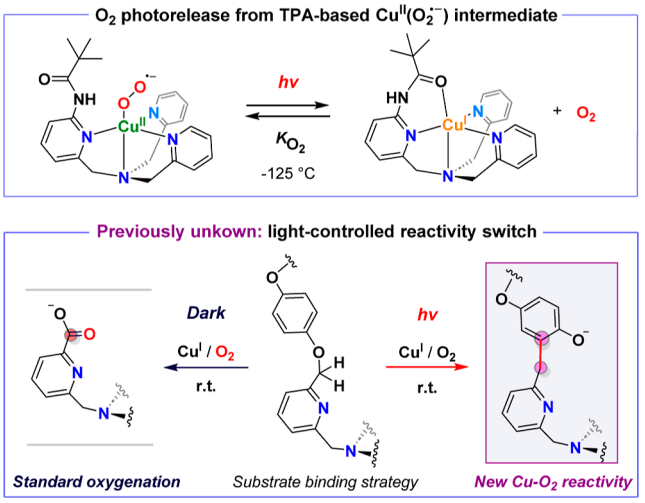

Figure 1. Previously reported photorelease of the O_2 from $Cu-O_2$ intermediates, hampering reactivity studies under irradiation (top). Yet unexplored reactivity switch of $Cu-O_2$ species induced by light (this work, bottom).

To probe the yet unexplored reactivity of $Cu-O_2$ species under irradiation, we reasoned that a closely positioned C−H substrate might promote HAA reactivity by $Cu(O_2^{\bullet-})$ prior to the O_2 photorelease. Substrate-binding Cu^I-complexes have been,[24−30] and are still currently[31] used as convenient tools to extend fundamental knowledge on the reactivity of $Cu-O_2$ intermediates. In this context, $PhO-CH_2$ substrates appear as appealing targets since (i) **TPA**-supported $Cu(O_2^{\bullet-})$ intermediates perform oxygenation of aryl alkyl ether bonds at room temperature,[32] and (ii) this reactivity was exploited to develop superoxide sensors.[33,34] Additionally, although aryl etheric C−H bonds are weaker than unactivated C_{sp3}-H bonds, they are found as robust linkages in several biomolecules, such as lignin.

We, therefore, designed and studied sophisticated "substrate-binding" catalysts based on the Cu(**TPA**) core, which is well-known for generating $Cu(O_2^{\bullet-})$ intermediates upon reaction of Cu^I precursors with O_2.[35−38] Following this strategy, we manage to obtain a key precedent for a light-induced reactivity switch in Cu^I-O_2 chemistry.

We derivatized the archetypal **TPA** scaffold by installing one aryl ether $^{MeO}PhO-CH_2-$ unit onto the 6-position of the **TPA**'s pyridine moieties to give the open ligand $\mathbf{L_1}$. A related cage **HmTPA**, recently studied in our group as Fe-ligand for selective oxidation of methane,[39,40] was also investigated featuring a single isolated copper-binding site (Figure 2). Interestingly, oxygenation studies on the new, open, and caged complexes $Cu^I(\mathbf{L_1})^+$ and $Cu^I(\mathbf{HmTPA})^+$, revealed a photo-induced [1,3]-shift rearrangement involving a C−O bond cleavage and the formation of a new C−C bond with the resulting phenolate unit. Reactivity studies and DFT (Density Functional Theory) calculations were combined to propose a reaction mechanism that supports the role of a cupric-superoxide primary intermediate. This represents, to the best of our knowledge, the first example of a light-induced switch of the Cu(**TPA**)/O_2 reactivity.

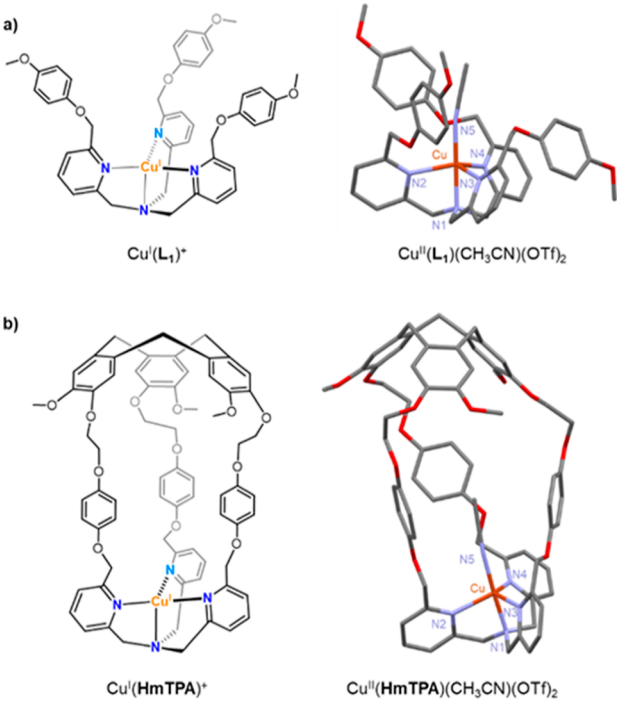

Figure 2. Representation of the Cu^I complexes used in this study along with views of the X-ray structures of corresponding copper(II) complexes based on (a) $\mathbf{L_1}$ and (b) **HmTPA** (adapted with permission from Ikbal A.; Colomban C.; Zhang D.; Delecluse M.; Brotin T.; Dufaud V.; Dutasta J.-P.; Sorokin A. B.; Martinez A. *Inorg. Chem.* **2019**, 58, 7220−7228. Copyright [2019] American Chemical Society).

RESULTS AND DISCUSSION

Characterization of the Cu-Catalysts

The new open and caged copper(I) complexes $Cu^I(\mathbf{L_1})(PF_6)$ and $Cu^I(\mathbf{HmTPA})(PF_6)$ have been prepared and characterized (Figures S11−S18). X-ray crystal structures of the related Cu^{II}-complexes $Cu^{II}(\mathbf{L_1})(OTf)_2$ and $Cu^{II}(\mathbf{HmTPA})(OTf)_2$[40] (Figure 2), revealed usual pentacoordinated Cu(II) centers in a trigonal bipyramidal geometries that comprise the **TPA** ligand and an axial molecule of CH_3CN in *trans* to the tertiary amine, as found in the archetypal $Cu^{II}(\mathbf{TPA})(CH_3CN)(OTf)_2$ complex.[41] The average $Cu-N_{pyridine}$ bond lengths for $Cu^{II}(\mathbf{L_1})(CH_3CN)(OTf)_2$ and $Cu^{II}(\mathbf{HmTPA})(CH_3CN)(OTf)_2$, found at 2.155 and 2.121 Å respectively, are significantly longer than in the unsubstituted **TPA**-based complex (2.042 Å),[41] implying a weakening of the pyridine-to-Cu donation.

The electronic influence of the $PhO-CH_2-$ substituents was further confirmed by comparing the $Cu^{II/I}$ redox potentials of our complexes with those of the parent **TPA**-based Cu complex (Table 1). Complexes based on $\mathbf{L_1}$ and **HmTPA** display quasi-reversible $Cu^{II/I}$ redox waves at respectively +35 and +40 mV vs $Fc^{+/0}$ (CH_3CN; 0.15 M NBu_4PF_6, Figures S21 and S22). These values are strongly shifted to more cathodic potentials compared to the unsubstituted $Cu^{II}(\mathbf{TPA})$ (−400 mV vs $Fc^{+/0}$),[42] indicating a strong impact of the $PhO-CH_2-$ substituents resulting in destabilization of the Cu^{II} oxidation state.

It is known that the instability of the Cu^{II} oxidation state reduces the affinity of the corresponding Cu^I complex for O_2.[43] In addition, increased steric hindrance around the metal core,

https://doi.org/10.1021/jacsau.4c00184
JACS Au 2024, 4, 1966−1974

Table 1. Half-Wave $Cu^{II/I}$ Reduction Potentials ($E_{1/2}$) for $Cu^{II}(L)(CH_3CN)(OTf)_2$ (L = L_1, HmTPA) and the Parent Cu^{II}(TPA) Complex[a]

$Cu^{II}(L)(CH_3CN)^{2+}$, L=	$E_{1/2}$ vs Fc^+/Fc^0 (mV)	reference
HmTPA	+40	this work
L_1	+35	this work
TPA	−400	42

[a] $E_{1/2} = (E_{Pc} + E_{Pa})/2$, reported vs $Fc^{+/0}$ in CH_3CN in the presence of the NBu_4PF_6 electrolyte.

due to the lowering of the fluxional ligand motion at low temperature, can also disfavor the formation of copper−oxygen intermediates.[43] As a consequence, O_2-binding and accumulation of a possible end-on superoxocopper(II) intermediate, could not be evidenced at low temperature in O_2-saturated solutions of $Cu^I(L_1)$ or Cu^I(**HmTPA**) in acetone, CH_2Cl_2 or THF (monitored by UV−visible at temperatures ranging from −105 to 0 °C). O_2 activation at our Cu^I-complexes was therefore studied at room temperature.

O_2 Activation Under Ambient Conditions

Interestingly, solutions of $Cu^I(L_1)(PF_6)$ in acetone, CH_2Cl_2, or THF turned from pale yellow to purple upon exposure to air or O_2 for 16 h under ambient light, at room temperature.

Slow diffusion of Et_2O to this O_2-exposed solution allowed for separation and isolation of a purple complex $Cu^{II}(L_1^{PhO})(PF_6)$ with 85% yield and one minor blue complex $Cu^{II}(L_1^{COO})(PF_6)$, isolated in 15% yield (Figure 3A). XRD-characterization of $Cu^{II}(L_1^{PhO})(PF_6)$ reveals the formation of a pentacoordinated copper complex with a geometry between trigonal bipyramidal and square pyramidal (τ_5 = 0.5), which comprises the **TPA** ligand and an intramolecular phenolate ligand, with a $Cu-O_{Phenolate}$ distance of 1.894 Å and an average $Cu-N_{Pyridine}$ distance of 2.148 Å (Figure 3B). Remarkably, the major product $Cu^{II}(L_1^{PhO})^+$, arises from an unusual modification of one of the $PhO-CH_2-$ moieties of the substrate. We observe the cleavage of the C−O bond and concomitant formation of a new C−C bond between the resulting phenolate and methylene units. ESI-HRMS analysis of $Cu^{II}(L_1^{PhO})(PF_6)$ revealed one set of signals at m/z = 760.2318 corresponding to [Cu + L_1 − 1]. The latter can be attributed to a copper(II) complex with a deprotonated monoanionic ligand, consistent with the presence of one phenolate substituent (Figure S23). Formation of a copper complex in the +2 oxidation state was further confirmed by electron-paramagnetic resonance (EPR) analysis, which exhibits the typical spectrum of a mononuclear Cu^{II} complex in rhombic symmetry (Figure 3B). UV−vis spectrum of $Cu^{II}(L_1^{PhO})(PF_6)$ exhibits typical $PhO^- \rightarrow Cu^{II}$ charge transfer transitions (LMCT) at 551 nm and d−d transitions at 686 nm (See ESI for computed transition densities).

Along with the major Cu^{II}-phenolate product, O_2 activation at $Cu^I(L_1)(PF_6)$ yielded a minor blue complex, $Cu^{II}(L_1^{COO})(PF_6)$ (Figure 3). The latter arises from the well-known $Cu(O_2^{\bullet-})$-dependent oxidative cleavage of internal aryl etheric C−H bond into a carboxylate moiety.[33,34] Its full characterization (Figures S24−S27), including XRD analysis (Figure 4), revealed a Cu^{II}(**TPA**)-based complex bound to an internal carboxylate unit with a $Cu-O^{carboxylate}$ distance of 1.972 Å. Furthermore, the formation of the product $Cu^{II}(^{18}O\text{-}L_1^{COO})$, incorporating one ^{18}O atom, was observed by performing the reaction under an ^{18}O-labeled O_2 atmosphere (Figure S49).

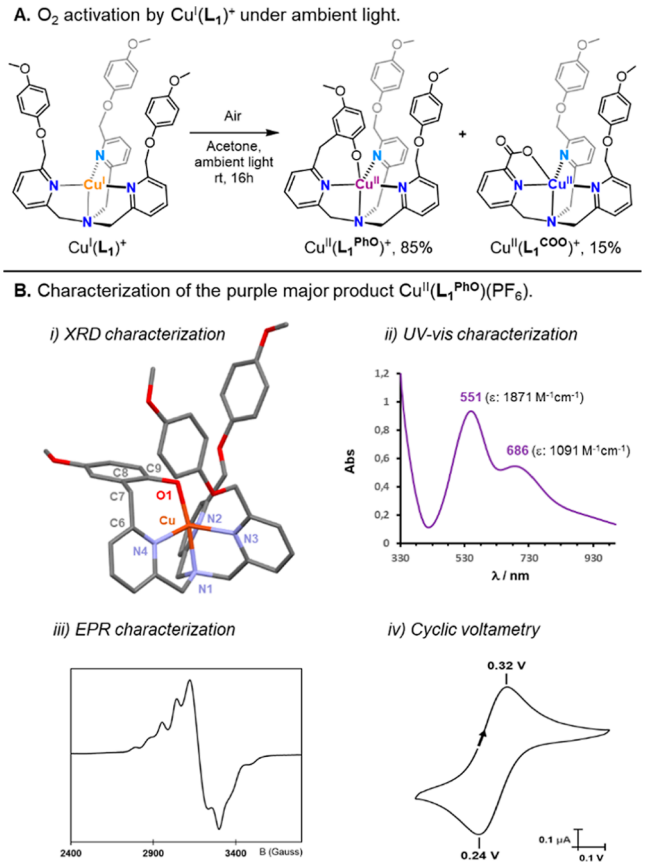

Figure 3. (A) Isolated products resulting from O_2 activation at $Cu^I(L_1)(PF_6)$ under ambient conditions. (B) View of the XRD crystal structure of the major purple product $Cu^{II}(L_1^{PhO})(PF_6)$ along with its UV−vis (0.5 mM in acetone), X-band EPR spectrum at 120 K (1 mM in acetone +5% CH_3CN) and cyclic voltammetry characterization (1.5 mM; 100 mV.s^{-1}; CH_3CN; 0.15 M NBu_4PF_6; platinum WE ⌀ = 2 mm; E vs Fc^+/Fc^0). (EPR: parameters extracted from simulation: g_1 = 2.008, g_2 = 2.100, g_3 = 2.245, and A_1^{Cu} = 235, A_2^{Cu} = 124, and A_3^{Cu} = 270 MHz).

This oxidative cleavage of one aryl-etheric arm into carboxylate is consistent with the initial formation of an aryl ester product $Cu^I(L_1{=}O)$ via aliphatic HAA. Oxygenation of the $PhO-CH_2-$ moiety by a superoxocopper(II) intermediate was previously proposed with calix-arene appended **TPA**-based complexes.[32]

Light-Induced Reactivity Switch

To probe the role of copper, O_2, and light in the particularly intriguing new reactivity of Cu^I-O_2 species, we performed control experiments under an inert atmosphere and/or dark conditions. As expected, our Cu^I complexes remain stable under an inert atmosphere, attesting to the crucial need of the O_2 oxidant to yield the phenolate products. Remarkably, when the reaction was performed in the dark, no purple product $Cu^{II}(L_1^{PhO})^+$ could be formed upon O_2 exposure of a solution of $Cu^I(L_1)(PF_6)$ at room temperature for 16 h.[44] Instead, the oxygenation reaction performed in the absence of light yielded almost equimolar amounts of the Cu^{II}-products $Cu^{II}(L_1^{COO})^+$ and $Cu^{II}(L_1)^{2+}$ (Figure 5).

To further investigate this crucial role of light, irradiation studies of an oxygenated solution of $Cu^I(L_1)(PF_6)$ have been performed at room temperature and monitored by UV−vis. Different irradiation wavelengths were selected using appro-

https://doi.org/10.1021/jacsau.4c00184
JACS Au 2024, 4, 1966−1974

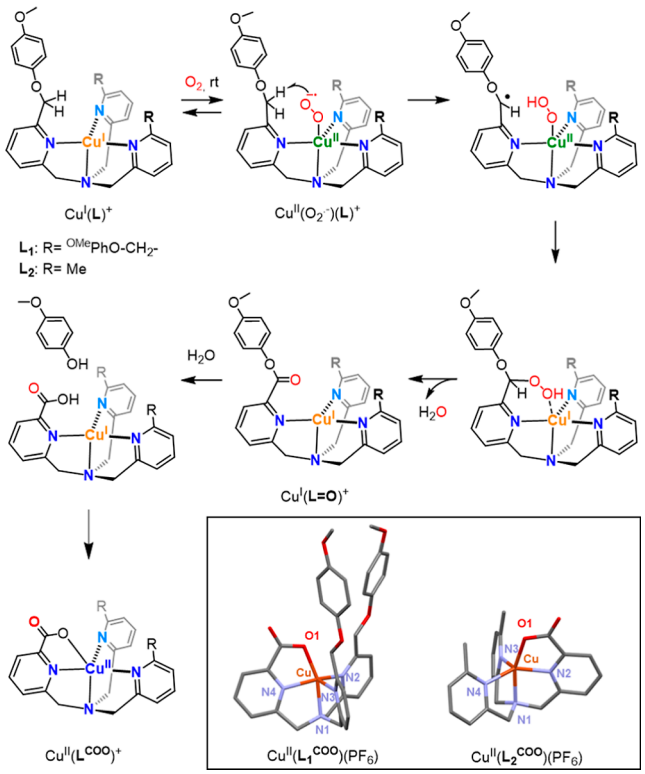

Figure 4. Proposed mechanism for the light-independent minor oxidative cleavage of PhO−CH_2 bond via O_2 activation at $Cu^I(\mathbf{L_1})^+$ and $Cu^I(\mathbf{L_2})^+$ yielding the Cu^{II}-carboxylate complexes $Cu^{II}(\mathbf{L_1}^{COO})(PF_6)$ and $Cu^{II}(\mathbf{L_2}^{COO})(PF_6)$, along with view of their XRD structures.

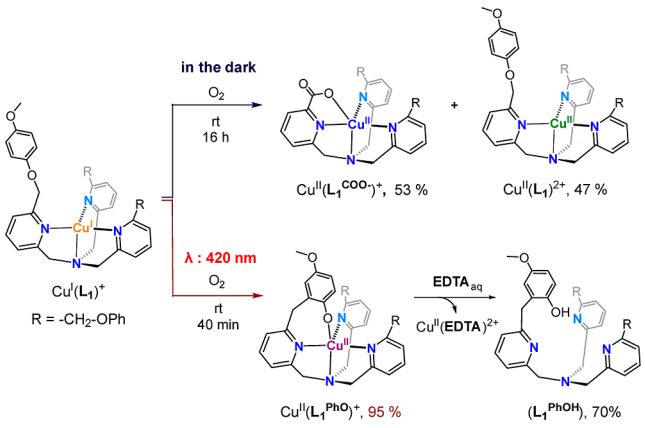

Figure 5. Products resulting from O_2 activation at $Cu^I(\mathbf{L_1})(PF_6)$ in the absence of light and under irradiation at 420 nm.

priate light filters mounted on a white source. No formation of Cu-phenolate product was observed under irradiation at $\lambda < 350$ and $\lambda > 490$ nm. Instead, irradiation of an oxygenated solution of $Cu^I(\mathbf{L_1})(PF_6)$ in THF, using $\lambda = 420$ nm (±10 nm), led to fast formation (40 min) of the purple product $Cu^{II}(\mathbf{L_1}^{PhO})(PF_6)$, attested by the appearance of the characteristic absorption band at 551 nm (Figure S41). Under these conditions, the activation of the O_2 at $Cu^I(\mathbf{L_1})^+$ results in the exclusive formation of the phenolate product with 95% isolated yield and without any formation of the oxygenation product $Cu^{II}(\mathbf{L_1}^{COO})^+$. These findings evidence a light-dictated switch in the reactivity of our Cu(**TPA**)-O_2 species. It is worth noting that $\mathbf{L_1}$ remains perfectly stable under the same conditions and in the absence of copper, demonstrating copper-dependent reactivity.

Importantly, this light-induced reactivity switch does not require the use of any additional photosensitizer. Moreover, it occurs under ambient light and an air atmosphere at room temperature. As a result, this mild and selective transformation of the aryl etheric PhO−CH_2− moiety into an *ortho*-substituted phenolate unit, represents a particularly convenient and straightforward way to access new phenol-based ligands. Accordingly, reaction of $\mathbf{L_1}$ with Cu^I and O_2 under irradiation at 420 nm in THF, followed by demetalation of the resulting purple product with EDTA, allows for the selective late-stage functionalization of the **TPA**-based ligand into the dissymmetric phenol-based ligand $\mathbf{L_1}^{PhOH}$ with high yields (Figures 5 and S42−S46). This strategy allows obtaining, in a single synthetical step, challenging heteroleptic coordinating structures, drastically facilitating the synthesis of enzyme-like nonsymmetrical binding pockets.

Formation of the Cu^{II}-phenolate product beyond the 50% yield threshold upon oxygenation of $Cu^{II}(\mathbf{L_1})^+$ (95% yield under irradiation at 420 nm), is a particularly intriguing new reactivity of Cu−O_2 species. Did this light-induced reactivity really occur at a single isolated copper center? To answer this question, we studied O_2 activation at the caged Cu^I(**HmTPA**)-(PF_6) complex that prevents formation of binuclear Cu_2O_2 intermediates. Interestingly, solutions of $Cu^I(\mathbf{HmTPA})(PF_6)$ in acetone, CH_2Cl_2, or THF also turned from pale yellow to purple upon exposure to air for 16 h, at room temperature and under ambient light. Slow diffusion of Et_2O to this air-exposed solution allowed isolation of the purple complex $Cu^{II}(\mathbf{HmTPA}^{PhO})(PF_6)$ with 80% yield. In this case, the formation of $Cu^{II}(\mathbf{HmTPA}^{PhO})(PF_6)$ was accompanied by the formation of a minor insoluble precipitate.

The purple product $Cu^{II}(\mathbf{HmTPA}^{PhO})(PF_6)$ displays similar cyclic voltammetry, EPR, and UV−vis signatures (Figures S37−S39) to those of the open analogue $Cu^{II}(\mathbf{L_1}^{PhO})(PF_6)$. Furthermore, ESI-HRMS analysis revealed one set of signals at m/z = 1204.3884 corresponding to [Cu + **HmTPA** − 1], which can be attributed to a copper(II) complex with a phenolate monoanionic ligand (Figure S40). Since our attempts to grow single crystals of $Cu^{II}(\mathbf{HmTPA}^{PhO})(PF_6)$ suitable for XRD analysis have remained unsuccessful, its structure has been proposed on the basis of DFT calculations and further confirmed using X-ray absorption spectroscopy (XAS) analysis. These characterizations were also performed with simpler benchmark complexes based on the ligand $\mathbf{L_2}$, an analogue of $\mathbf{L_1}$ in which two PhO−CH_2− arms have been replaced by methyl substituents to significantly decrease the shell scattering offered by the ligand.[45] XANES spectra were first recorded with the $\mathbf{L_1}$-based Cu-complexes $Cu^I(\mathbf{L_1})(PF_6)$, $Cu^{II}(\mathbf{L_1})(OTf)_2$ and $Cu^{II}(\mathbf{L_1}^{PhO})(PF_6)$ (Figure 6B*i*). $Cu^I(\mathbf{L_1})$-(PF_6) shows the typical feature at 8982.5 eV due to 1s-4p transitions and shakedown contributions indicative of Cu^I centers having a vacant axial coordination site, while $Cu^{II}(\mathbf{L_1})(OTf)_2$ and $Cu^{II}(\mathbf{L_1}^{PhO})(PF_6)$ show a weak 1s-3d transition at 8978.7 eV typical of Cu(II) centers.[46,47] More importantly, the EXAFS signal of $Cu^{II}(\mathbf{L_1}^{PhO})(PF_6)$ displays, in the 2−3 Å range of the FT transformed spectra, a clear increase in intensity consistent with the additional scattering expected from the coordination of the phenolate and formation of the seven-membered ring, when compared to the Cu^{II} analogue (Figure 6B*i*). This is even more clearly seen in the $Cu^{II}(\mathbf{L_2}^{PhO})(PF_6)$ sister complex, in which only one

https://doi.org/10.1021/jacsau.4c00184
JACS Au 2024, 4, 1966−1974

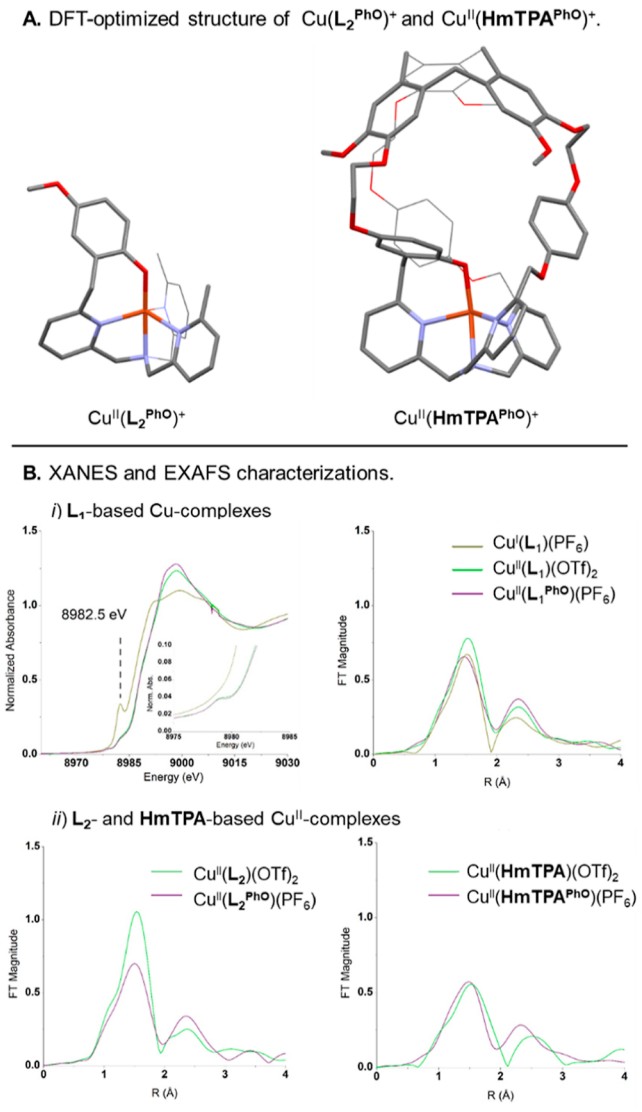

Figure 6. (A) Views of the DFT-optimized structure (CAMB3LYP-D3/def2-TZVP) of $Cu^{II}(\mathbf{L}^{PhO})^+$ (L = $\mathbf{L}_2$ or **HmTPA**). (B*i*) XANES with inset showing the pre-edge region (left) and Fourier transformed EXAFS spectra of $Cu^{I}(\mathbf{L}_1)$, $Cu^{II}(\mathbf{L}_1)$, and $Cu^{II}(\mathbf{L}_1^{PhO})$ complexes (right). (B*ii*) EXAFS Fourier transformed spectra of $Cu^{II}(\mathbf{L})$ and $Cu^{II}(\mathbf{L}^{PhO})$ complexes (L = $\mathbf{L}_2$ (left) or **HmTPA** (right); see ESI for full XAS characterization).

PhO−CH_2−pyridine moiety is present, with more pronounced changes in higher shell scattering due to the Cu-phenolate resulting structure (Figure 6B*ii*). Similar results are obtained for the caged $Cu^{II}(\mathbf{HmTPA}^{PhO})(PF_6)$ complex, however with more modest changes in the scattering shell centered at 2.5 Å, primarily due to the existing cage structure, which already contributes to the scattering in the $Cu^{II}(\mathbf{HmTPA})(OTf)_2$ parent compound (Figure 6B*ii*). Formation of the Cu^{II}-phenolate complex at $\mathbf{HmTPA}^{PhO}$ was further corroborated by its optimized DFT structure (Figure 6A) that reveals Cu^{II}-coordination modes very similar to the one observed in the XRD structure of $Cu^{II}(\mathbf{L}_1^{PhO})(PF_6)$. The fact that this previously unknown dioxygen- and light-induced reactivity occurs at the single isolated Cu site of $Cu^{I}(\mathbf{HmTPA})^+$, clearly suggests the involvement of a mononuclear Cu−O_2 adduct.

Redox Properties of the Cu^{II}−Phenolate Products

The straightforward preparation of new Cu^{II}-phenolate complexes permit the access to crucial targets in bioinspired chemistry, due to their ability to generate copper-coordinated phenoxyl radical.[48,49] Such metal-radical species play a crucial role in O_2-activating copper oxidase enzymes such as galactose oxidase (GO).[50−52]

Interestingly, no reduction processes were observed with the Cu^{II}-phenolate products $Cu^{II}(\mathbf{L}_1^{PhO})(PF_6)$ and $Cu^{II}(\mathbf{HmTPA}^{PhO})(PF_6)$. Instead, their cyclic voltammograms exhibit quasi-reversible oxidation processes at, respectively, +270 and +320 mV vs $Fc^{+/0}$ (Figures 3B and S37). These oxidation processes could be attributed to metal- (Cu^{II}/Cu^{III}) or ligand-centered (phenolate/phenoxyl radical) oxidation processes. To elucidate the nature of the oxidized species, the chemical oxidation of the Cu^{II}-phenolate complexes was performed. Because the oxidized products were found to be insufficiently stable at rt, chemical oxidations were performed at low temperature. We first investigated the use of the $Cu^{II}(OTf)_2$ salt as oxidizing agent (reported formal potential of 400 mV vs $Fc^{+/0}$).[53] Addition of 1.2 equiv of this oxidant to a 0.5 mM acetone solution of $Cu^{II}(\mathbf{L})(PF_6)$ (L = $\mathbf{L}_1^{PhO}$ or $\mathbf{HmTPA}^{PhO}$) at −85 °C results in changes in the UV−vis spectra suggesting the successful formation of oxidized complexes that remain stable several hours at this temperature. The typical UV−vis signature of the starting **L**-Cu^{II}-phenolate complexes disappears to the profit of a more intense band centered at 475 nm (λ = 3780 M^{-1} cm^{-1}) (Figure 7).

A similar result is obtained with $Cu^{II}(\mathbf{HmTPA}^{PhO})(PF_6)$ (Figure S47). The absorption maximum and intensity of this band in the oxidized complex $Cu^{II}(\mathbf{L}^{PhO\bullet})(PF_6)^+$ (**L** = $\mathbf{L}_1$ or **HmTPA**), are in good agreement with the values reported for related Cu^{II}-phenoxyl radical complexes,[50] suggesting a

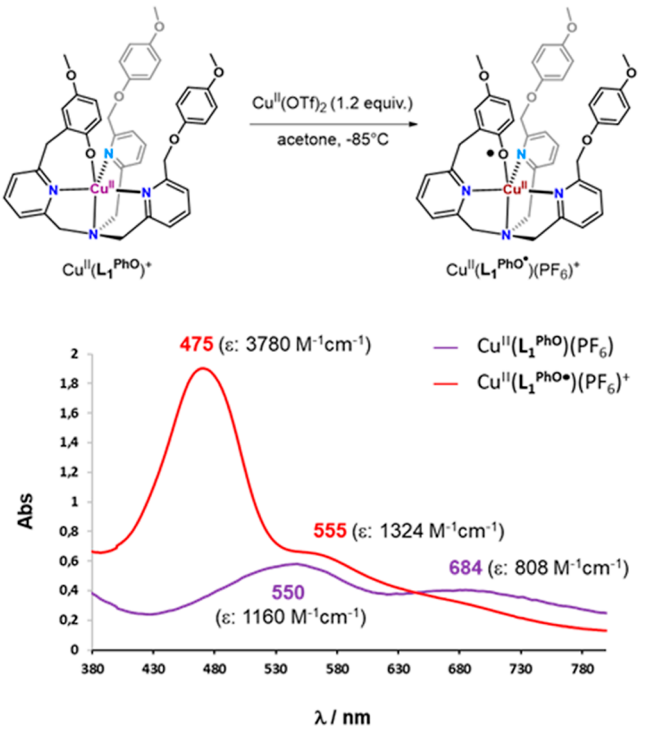

Figure 7. Absorption spectral change upon addition of $Cu^{II}(OTf)_2$ (1.2 equiv) to a 0.5 mM solution of $Cu^{II}(\mathbf{L}_1^{PhO})(PF_6)$ in acetone at −85 °C.

https://doi.org/10.1021/jacsau.4c00184
JACS Au 2024, 4, 1966−1974

phenolate-centered oxidation process. Formation of $Cu^{II}(\mathbf{HmTPA}^{PhO\bullet})^{2+}$ can also take place in the presence of the stronger oxidant ammonium cerium(IV) nitrate (CAN) under identical conditions, yielding the same UV−vis signatures (Figure S48).[54] Furthermore, frozen solutions of $Cu^{II}(\mathbf{L}^{PhO\bullet})(PF_6)^+$ were studied by EPR and XANES spectroscopies. The oxidation of the Cu^{II}-phenolate complexes resulted in the loss of their X-band EPR signal, which was compatible with the formation of magnetically coupled Cu^{II}−$PhO^\bullet$ complexes. Finally, XANES characterization of $Cu^{II}(\mathbf{HmTPA}^{PhO\bullet})(PF_6)^+$, generated in the presence of CAN, confirmed the absence of a Cu^{III} complex, as evidenced by the presence of pre-edge and rising edge energies overlapping those of the $Cu^{II}(\mathbf{HmTPA}^{PhO})(PF_6)$ parent complex. The latter further supports a ligand-centered oxidation process (Figure XAS3). To the best of our knowledge, this represents the first evidence of generation of **TPA**-based Cu^{II}-phenoxyl radical species within a cage-like ligand.

Proposed Mechanism for the New Light-Induced Cu(TPA)/O_2 Reactivity

The extensively documented activation of O_2 at tetradentate $Cu^I(\mathbf{TPA})$ derivatives supports the initial generation of highly reactive superoxide intermediates $Cu^{II}(\mathbf{TPA})(O_2^{\bullet-})$ that could either convert to peroxodicopper(II) complexes or undergo HAA from C−H bond substrates.[7−13,32] Furthermore, we demonstrated that (i) our light-directed rearrangement of aryl-ether bonds proceeds with high yields (>95%), above the 50% threshold expected for binuclear mechanism, and (ii) the reaction occurs at isolated O_2-activating Cu^I site in $Cu^I(\mathbf{HmTPA})^+$. To provide additional experimental evidence supporting a cupric-superoxide-dependent reaction, and inspired by the previous studies of aryl ether appended $Cu^{II}(\mathbf{TPA})$ superoxide sensors,[33,34] reaction of the copper(II) complex $Cu^{II}(\mathbf{L_1})(OTf)_2$, with potassium superoxide (KO_2) was studied under light. Interestingly, while no formation of the phenolate-Cu^{II} product could be observed in the dark, reacting $Cu^{II}(\mathbf{L_1})(OTf)_2$ with KO_2 (10 equiv), under light, gives $Cu^{II}(\mathbf{L_1}^{PhO})(OTf)$ in a c.a. 30% yield (Figures S50 and S51). This lower yield, compared to the Cu^I/O_2 driven reactivity, might arise from partial superoxide decomposition in DMSO. Importantly, no formation of $Cu^{II}(\mathbf{L_1}^{PhO})(OTf)$ could be observed upon reacting the starting Cu^{II}-complex with 10 equiv of ^{tBu}OOH, H_2O_2, or an H_2O_2: Et_3N 1:1 mixture, under light (Figure S52). Altogether, these findings strongly support a $Cu^{II}(O_2^{\bullet-})$-dependent reactivity.

Based on these experimental results, a theoretical treatment was performed to propose a reaction pathway for the activation of O_2 with $Cu^I(\mathbf{L})^+$ complexes (**L** = $\mathbf{L_1}$, $\mathbf{L_2}$ or **HmTPA**), which results in the formation of the phenolate products (Scheme 1). The most probable initial step is the formation of the end-on Cu^{II}-superoxide complex $Cu^{II}(\mathbf{L})(O_2^{\bullet-})^+$.

Then, an intramolecular HAA of the proximal aryl etheric HC−H bond occurs, leading to intermediate **I**, which displays a $HC^\bullet$ radical stabilized by the pyridine. The release of the resulting OOH ligand is necessary to reach the final product, and this may readily occur to form **II** (see Supporting Information pages S45−S65). From here, the phenolated product would be obtained, on the ground state (GS) potential energy surface, in a three-step mechanism.[55] First, C−C bond formation leads to intermediate **III**. Then **IV** is obtained through the cleavage of the C−O bond. The phenolate

Scheme 1. Mechanistic Proposal. $\Delta\Delta E$ (kcal/mol, PBE0-D3/def2-ZTVP) are Electronic Energy Differences Relative to the Previous Minimum, Indicated as a Subscript. $\Delta\Delta E^{\#}$ (kcal/mol) are Energy Barriers

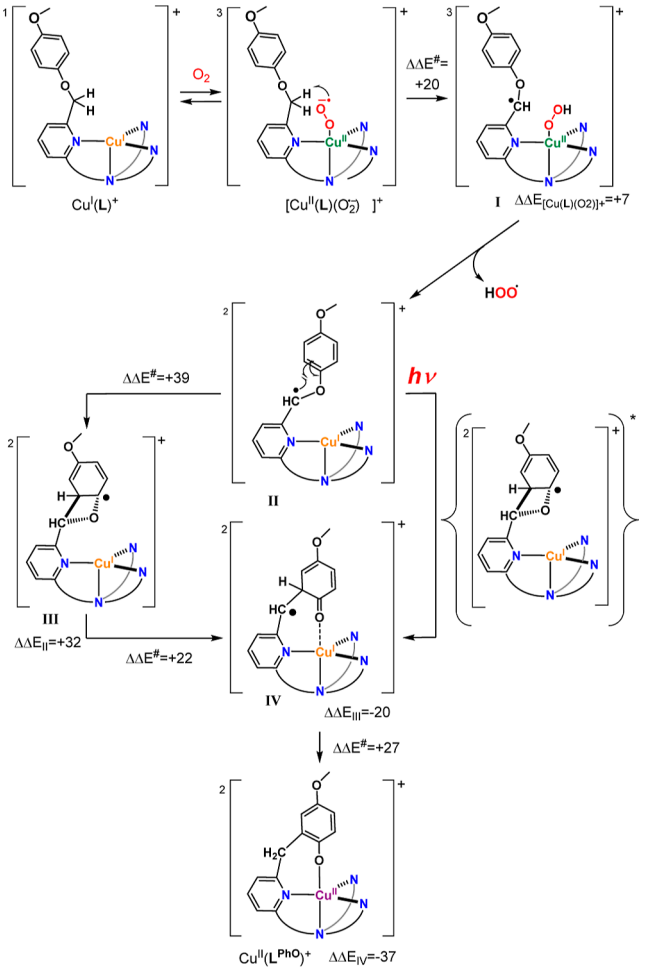

product is finally reached in a rearomatization step. The GS calculations reveal that the energetically demanding steps are the C−C bond formation (barrier of $\Delta\Delta E$# = 39 kcal/mol in total electronic energy, with respect to **II**, PBE0-D3/def2-ZTVP) and, even more, the C−O bond cleavage (barrier of $\Delta\Delta E^{\#}$ = 22 kcal/mol in total electronic energy, with respect to **III**). The overall energy cost from **II** to the **IV** is of 54 kcal/mol (energies difference between the transition state leading from **III** to **IV**, and **II**) and cannot be overcome at room temperature. This confirms that the photochemical pathway allows the avoidance of these steps.

TDDFT calculations reveal that intermediates **I** and **II** display absorptions at 414 and 381 nm, respectively (CAMB3LYP-D3 values), which are compatible with the experimental findings that the reaction is promoted upon irradiation at *ca.* λ = 420 nm. Preliminary calculations on the ground and excited state potential energy surface suggest that, indeed, there exist reaction paths on the excited potential energy surface that lead to **IV** from **II** by circumventing the high C−O cleavage barrier (see Supporting Information). Altogether, calculations confirm that the photoirradiated mechanistic proposal depicted in Scheme 1, which could be considered as an unexpected formal [1,3]-shift rearrangement[56] promoted by the initial HAA from Cu−O_2 species, is

https://doi.org/10.1021/jacsau.4c00184
JACS Au 2024, 4, 1966−1974

feasible from both kinetic and thermodynamic views. These results indicate that irradiation might provide a new path for the reaction of the substrate radical ($R^{\bullet}$) generated upon HAA by cupric superoxide. Irradiation might favor rebound of $R^{\bullet}$ with the aryl unit over its rebound with the hydroperoxide intermediate (prevailing mechanism for the light-independent oxygenation reactivity).

CONCLUSIONS

The extensive reactivity studies on bioinspired $Cu^{II}(O_2^{\bullet-})$(**TPA**)-based intermediates have demonstrated the remarkable oxidation reactivity of their ground states. Using light to tune the reactivity of $Cu-O_2$ species is a formidable opportunity given the abundance of cupric-superoxide intermediates in enzymatic active sites. So far, exploration of $Cu-O_2$ reactivity under irradiation has been hampered by the photorelease of O_2. In this report, we provide a key precedent for a light-induced reactivity switch in $Cu(I)-O_2$ chemistry, by positioning C−H substrates in close proximity to the active site. We have found that activation of the O_2 at the Cu^{I}(**TPA**) core, via probable cupric-superoxide intermediates, results in an unprecedented light-induced reactivity toward aryl ether internal substrates. Detailed analysis of the final products (including rare examples of XRD characterized compounds), demonstrated a light-dictated switch from standard C−H oxygenation to unusual [1,3]-shift rearrangement. This transformation does not require the use of any additional photosensitizer and even occurs under ambient light and air atmosphere at room temperature, with remarkably high yields. Both rate and selectivity of the reaction are drastically improved upon irradiation at λ = 420 nm compared to ambient light. Experimental evidence, combined with DFT calculations, indicates that the reaction occurs at isolated single $Cu-O_2$ sites and proceeds via sequential C−O cleavage and C−C bond formation in the excited state. The latter suggests that light might open new paths for the rebound of the substrate radical ($R^{\bullet}$) generated upon HAA by cupric superoxide. This unprecedented light-dictated reactivity provides considerable new insights into the new and exciting research area of metal-O_2 reactions under irradiation.[20−23] As speculated,[22,23] we demonstrated that energetically demanding steps (that cannot be overcome at room temperature on the ground state), could be avoided under irradiation, opening new overall reactivities initiated by $Cu-O_2$ intermediates. This quasi-quantitative transformation promoted by a combination of Cu, O_2, and light, provides a straightforward access for direct postfunctionalization of **TPA** derivatives, smoothing drastically the synthesis of enzyme-like nonsymmetrical binding pockets.

We envision that the present results, beyond improving fundamental knowledge of Cu-dioxygen reactivity, will find some crucial application in the field of copper catalysis. In particular, aryl ether linkages are important targets found in numerous biomolecules as lignin.[57] Future work in our laboratory will be devoted to the transfer of this reactivity toward external substrates.

METHODS

Instrumentation

^{1}H NMR and ^{13}C NMR were recorded on a Bruker Avance III HD 300 and 500 MHz spectrometers. ^{1}H NMR and ^{13}C NMR chemical shifts δ are reported in parts per million referenced to the protonated residual solvent signal. ESI-HRMS were performed on a SYNAPT G2 HDMS (Waters) mass spectrometer with API and spectra were obtained with TOF analysis. Measurements were realized with two internal standards.

Electrochemical experiments were recorded on a Bio-logic SP-150 potentiostat equipped with EC-Lab software. Cyclic voltammetry experiments were conducted in the presence of NBu_4PF_6 as supporting electrolyte and using three-electrode setup which consisted of a Pt working electrode (1.6 mm), a platinum wire counter electrode, and a leakless AgCl/Ag reference electrode (EDAQ). The potentials in the text are referenced versus Fc^+/Fc^0.

X-band EPR spectra were recorded by using a Bruker ELEXSYS cw-EPR instrument equipped with a BVT 3000 digital temperature controller. The spectra were recorded at 120 K in frozen solutions. Typical parameters were: microwave power 10−20 mW, modulation frequency 100 kHz, and modulation gain 3 G. EPR spectra were simulated using the EasySpin toolbox developed for Matlab (Stoll, S.; Schweiger, A., 2006. EasySpin, a comprehensive software package for spectral simulation and analysis in EPR. J. Magn. Res. 178, 42−55).

UV−vis spectroscopic experiments were performed by using a JASCO V-730ST UV/vis Spectrophotometer equipped with a UNISOKU cryostat.

ASSOCIATED CONTENT

Supporting Information

The Supporting Information is available free of charge at https://pubs.acs.org/doi/10.1021/jacsau.4c00184.

General information; detailed experimental procedure for the synthesis of ligands and Cu complexes; procedures for O_2 activation studies; full characterization of newly characterized products; XRD characterizations; XAS studies; computational study details; computed absorption spectra; computed mechanism on the ground potential energy surface; preliminary TDDFT computational studies on excited state surfaces (PDF)

AUTHOR INFORMATION

Corresponding Authors

Cédric Colomban − *Aix Marseille Univ, CNRS, Centrale Marseille, 13013 Marseille, France;* orcid.org/0000-0002-6862-4173; Email: cedric.colomban@univ-amu.fr

Alexandre Martinez − *Aix Marseille Univ, CNRS, Centrale Marseille, 13013 Marseille, France;* orcid.org/0000-0002-6745-5734; Email: alexandre.martinez@centralemarseille.fr

A. Jalila Simaan − *Aix Marseille Univ, CNRS, Centrale Marseille, 13013 Marseille, France;* orcid.org/0000-0003-2537-0422; Email: jalila.simaan@univ-amu.fr

Paola Nava − *Aix Marseille Univ, CNRS, Centrale Marseille, 13013 Marseille, France;* orcid.org/0000-0002-8909-8002; Email: paola.nava@univ-amu.fr

Authors

Donglin Diao − *Aix Marseille Univ, CNRS, Centrale Marseille, 13013 Marseille, France*

Anna Baidiuk − *Aix Marseille Univ, CNRS, Centrale Marseille, 13013 Marseille, France*

Leo Chaussy − *Aix Marseille Univ, CNRS, Centrale Marseille, 13013 Marseille, France;* orcid.org/0000-0001-6357-9062

Iago De Assis Modenez − *Aix Marseille Univ, CNRS, Centrale Marseille, 13013 Marseille, France*

Xavi Ribas − *Institut de Quimica Computacional i Catalisi (IQCC), Departament de Quimica, Universitat de Girona, Girona E-17003 Catalonia, Spain;* orcid.org/0000-0002-2850-4409

Marius Réglier − *Aix Marseille Univ, CNRS, Centrale Marseille, 13013 Marseille, France*
Vlad Martin-Diaconescu − *ALBA Synchrotron, Barcelona 08290, Spain*

Complete contact information is available at: https://pubs.acs.org/10.1021/jacsau.4c00184

Author Contributions

‖D.D. and A.B. contributed equally.

Notes

The authors declare no competing financial interest.

■ ACKNOWLEDGMENTS

This work received support from the French government under the France 2030 investment plan, as part of the "Initiative d'Excellence d'Aix-Marseille Université" − A*MIDEX (AMX-21- PEP-041). This work was supported by ANR-22-CE50-0009-01. X.R. thanks financial support from PID2022-136970NB-I00 (MINECO-Spain) and ICREA-Academia. Experiments were performed at CLAESS beamline at ALBA Synchrotron with the collaboration of ALBA staff as part of proposal 2022025630. We thank the "Centre de Calcul Intensif d'Aix-Marseille" for granting us access to its high-performance computing resources (project b288).

■ REFERENCES

(1) Fukuzumi, S.; Lee, Y.-M.; Nam, W. Structure and reactivity of the first-row d-block metal-superoxo complexes. *Dalton Trans.* **2019**, *48*, 9469−9489.
(2) Osborne, R. L.; Klinman, J. P. *Copper-Oxygen Chemistry* Karlin, K. D., Itoh, S., Eds.; John Wiley & Sons, Inc: Hoboken, 2011; p 1.
(3) Solomon, E. I.; Heppner, D. E.; Johnston, E. M.; Ginsbach, J. W.; Cirera, J.; Qayyum, M.; Kieber-Emmons, M. T.; Kjaergaard, C. H.; Hadt, R. G.; Tian, L. Copper Active Sites in Biology. *Chem. Rev.* **2014**, *114*, 3659−3853.
(4) Elwell, C. E.; Gagnon, N. L.; Neisen, B. D.; Dhar, D.; Spaeth, A. D.; Yee, G. M.; Tolman, W. B. Copper−Oxygen Complexes Revisited: Structures, Spectroscopy, and Reactivity. *Chem. Rev.* **2017**, *117*, 2059−2107.
(5) Trammell, R.; Rajabimoghadam, K.; Garcia-Bosch, I. Copper-Promoted Functionalization of Organic Molecules: from Biologically Relevant Cu/O_2 Model Systems to Organometallic Transformations. *Chem. Rev.* **2019**, *119* (4), 2954−3031.
(6) Kim, B.; Karlin, K. D. Ligand−Copper(I) Primary O_2-Adducts: Design, Characterization, and Biological Significance of Cupric−Superoxides. *Acc. Chem. Res.* **2023**, *56*, 2197−2212.
(7) Itoh, S. Developing Mononuclear Copper−Active-Oxygen Complexes Relevant to Reactive Intermediates of Biological Oxidation Reactions. *Acc. Chem. Res.* **2015**, *48*, 2066−2074.
(8) Keown, W.; Gary, J. B.; Stack, T. D. P. High-valent copper in biomimetic and biological oxidations. *J. Biol. Inorg. Chem.* **2017**, *22*, 289−305.
(9) Quist, D. A.; Diaz, D. E.; Liu, J. J.; Karlin, K. D. Activation of dioxygen by copper metalloproteins and insights from model complexes. *J. Biol. Inorg. Chem.* **2017**, *22*, 253−288.
(10) Würtele, C.; Gaoutchenova, E.; Harms, K.; Holthausen, M. C.; Sundermeyer, J.; Schindler, S. Crystallographic Characterization of a Synthetic 1:1 End-On Copper Dioxygen Adduct Complex. *Angew. Chem., Int. Ed.* **2006**, *45*, 3867−3869.
(11) Bailey, W. D.; Dhar, D.; Cramblitt, A. C.; Tolman, W. B. Mechanistic Dichotomy in Proton-Coupled Electron-Transfer Reactions of Phenols with a Copper Superoxide Complex. *J. Am. Chem. Soc.* **2019**, *141*, 5470−5480.
(12) Pirovano, P.; Magherusan, A. M.; McGlynn, C.; Ure, A.; Lynes, A.; McDonald, A. R. Nucleophilic Reactivity of a Copper(II)−Superoxide Complex. *Angew. Chem., Int. Ed.* **2014**, *126*, 6056−6060.
(13) Abe, T.; Hori, Y.; Shiota, Y.; Ohta, T.; Morimoto, Y.; Sugimoto, H.; Ogura, T.; Yoshizawa, K.; Itoh, S. Cupric-superoxide complex that induces a catalytic aldol reaction-type C−C bond formation. *Commun. Chem.* **2019**, *2* (1), 12.
(14) Mills, I. N.; Porras, J. A.; Bernhard, S. Judicious Design of Cationic, Cyclometalated Ir(III) Complexes for Photochemical Energy Conversion and Optoelectronics. *Acc. Chem. Res.* **2018**, *51*, 352−364.
(15) Li, T.-Y.; Wu, J.; Wu, Z.-G.; Zheng, Y.-X.; Zuo, J.-L.; Pan, Y. Rational design of phosphorescent iridium(III) complexes for emission color tunability and their applications in OLEDs. *Coord. Chem. Rev.* **2018**, *374*, 55−92.
(16) Perutz, R. N.; Procacci, B. Photochemistry of Transition Metal Hydrides. *Chem. Rev.* **2016**, *116*, 8506−8544.
(17) Kuninobu, Y.; Takai, K. Organic Reactions Catalyzed by Rhenium Carbonyl Complexes. *Chem. Rev.* **2011**, *111*, 1938−1953.
(18) Sun, Q.; Mosquera-Vazquez, S.; Suffren, Y.; Hankache, J.; Amstutz, N.; Lawson Daku, L. M.; Vauthey, E.; Hauser, A. On the role of ligand-field states for the photophysical properties of ruthenium(II) polypyridyl complexes. *Coord. Chem. Rev.* **2015**, *282*−*283*, 87−99.
(19) Reichle, A.; Reiser, O. Light-induced homolysis of copper(II)-complexes − a perspective for photocatalysis. *Chem. Sci.* **2023**, *14*, 4449−4462.
(20) Sharma, N.; Jung, J.; Ohkubo, K.; Lee, Y.-M.; El-Khouly, M. E.; Nam, W.; Fukuzumi, S. Long-Lived Photoexcited State of a Mn(IV)-Oxo Complex Binding Scandium Ions That is Capable of Hydroxylating Benzene. *J. Am. Chem. Soc.* **2018**, *140*, 8405−8409.
(21) Saracini, C.; Ohkubo, K.; Suenobu, T.; Meyer, G. J.; Karlin, K. D.; Fukuzumi, S. Laser-Induced Dynamics of Peroxodicopper(II) Complexes Vary with the Ligand Architecture. One-Photon Two-Electron O_2 Ejection and Formation of Mixed-Valent $Cu^{I}Cu^{II}$−Superoxide Intermediates. *J. Am. Chem. Soc.* **2015**, *137*, 15865−15874.
(22) Saracini, C.; Fukuzumi, S.; Lee, Y.-M.; Nam, W. Photoexcited state chemistry of metal−oxygen complexes. *Dalton Trans.* **2018**, *47*, 16019−16026.
(23) Saracini, C.; Liakos, D. G.; Zapata Rivera, J. E.; Neese, F.; Meyer, G. J.; Karlin, K. D. Excitation Wavelength Dependent O_2 Release from Copper(II)−Superoxide Compounds: Laser Flash-Photolysis Experiments and Theoretical Studies. *J. Am. Chem. Soc.* **2014**, *136*, 1260−1263.
(24) Kunishita, A.; Kubo, M.; Sugimoto, H.; Ogura, T.; Sato, K.; Takui, T.; Itoh, S. Mononuclear Copper(II)−Superoxo Complexes that Mimic the Structure and Reactivity of the Active Centers of PHM and DβM. *J. Am. Chem. Soc.* **2009**, *131*, 2788−2789.
(25) Blain, I.; Bruno, P.; Giorgi, M.; Lojou, E.; Lexa, D.; Réglier, M. Copper Complexes as Functional Models for Dopamine β-Hydroxylase − Stereospecific Oxygen Atom Transfer. *Eur. J. Inorg. Chem.* **1998**, *9*, 1297−1304.
(26) See, Y. Y.; Herrmann, A. T.; Aihara, Y.; Baran, P. S. Scalable C−H Oxidation with Copper: Synthesis of Polyoxypregnanes. *J. Am. Chem. Soc.* **2015**, *137*, 13776−13779.
(27) Schonecker, B.; Zheldakova, T.; Liu, Y.; Kotteritzsch, M.; Gunther, W.; Gorls, H. Biomimetic Hydroxylation of Nonactivated CH_2 Groups with Copper Complexes and Molecular Oxygen. *Angew. Chem., Int. Ed.* **2003**, *42*, 3240−3244.
(28) Izzet, G.; Zeitouny, J.; Akdas-Killig, H.; Frapart, Y.; Ménage, S.; Douziech, B.; Jabin, I.; Le Mest, Y.; Reinaud, O. Dioxygen Activation at a Mononuclear Cu(I) Center Embedded in the Calix[6]arene-Tren Core. *J. Am. Chem. Soc.* **2008**, *130*, 9514−9523.
(29) Becker, J.; Gupta, P.; Angersbach, F.; Tuczek, F.; Näther, C.; Holthausen, M. C.; Schindler, S. Selective Aromatic Hydroxylation with Dioxygen and Simple Copper Imine Complexes. *Chem.-Eur. J.* **2015**, *21*, 11735−11744.

(30) Becker, J.; Zhyhadlo, Y. Y.; Butova, E. D.; Fokin, A. A.; Schreiner, P. R.; Förster, M.; Holthausen, C.; Specht, P.; Schindler, S. Aerobic Aliphatic Hydroxylation Reactions by Copper Complexes: A Simple Clip-and-Cleave Concept. *Chem.-Eur. J.* **2018**, *24*, 15397−15549.
(31) Kim, B.; Brueggemeyer, M. T.; Transue, W. J.; Park, Y.; Cho, J.; Siegler, M. A.; Solomon, E. I.; Karlin, K. D. Fenton-like Chemistry by a Copper(I) Complex and H_2O_2 Relevant to Enzyme Peroxygenase C−H Hydroxylation. *J. Am. Chem. Soc.* **2023**, *145*, 11735−11744.
(32) Thiabaud, G.; Guillemot, G.; Schmitz-Afonso, I.; Colasson, B.; Reinaud, O. Solid-State Chemistry at an Isolated Copper(I) Center with O_2. *Angew. Chem., Int. Ed.* **2009**, *48*, 7383−7386.
(33) Yu, Z. H.; Chung, C. Y.-S.; Tang, F. K.; Brewer, T. F.; Au-Yeung, H. Y. A modular trigger for the development of selective superoxide probes. *Chem. Commun.* **2017**, *53*, 10042−10045.
(34) Tong, K. Y.; Zhao, J.; Tse, C.-W.; Wan, P.-K.; Rong, J.; Au-Yeung, H. Y. Selective catecholamine detection in living cells by a copper-mediated oxidative bond cleavage. *Chem. Sci.* **2019**, *10*, 8519−8526.
(35) Peterson, R. L.; Himes, R. A.; Kotani, H.; Suenobu, T.; Tian, L.; Siegler, M. A.; Solomon, E. I.; Fukuzumi, S.; Karlin, K. D. Cupric Superoxo-Mediated Intermolecular C−H Activation Chemistry. *J. Am. Chem. Soc.* **2011**, *133*, 1702−1705.
(36) Bhadra, M.; Lee, J. Y. C.; Cowley, R. E.; Kim, S.; Siegler, M. A.; Solomon, E. I.; Karlin, K. D. Intramolecular Hydrogen Bonding Enhances Stability and Reactivity of Mononuclear Cupric Superoxide Complexes. *J. Am. Chem. Soc.* **2018**, *140*, 9042−9045.
(37) Diaz, D. E.; Quist, D. A.; Herzog, A. E.; Schaefer, A. W.; Kipouros, I.; Bhadra, M.; Solomon, E. I.; Karlin, K. D. Impact of Intramolecular Hydrogen Bonding on the Reactivity of Cupric Superoxide Complexes with O−H and C−H Substrates. *Angew. Chem., Int. Ed.* **2019**, *58*, 17572−17576.
(38) Quek, S. Y.; Debnath, S.; Laxmi, S.; van Gastel, M.; Krämer, T.; England, J. Sterically Stabilized End-On Superoxocopper(II) Complexes and Mechanistic Insights into Their Reactivity with O−H, N−H, and C−H Substrates. *J. Am. Chem. Soc.* **2021**, *143*, 19731−19747.
(39) Diao, D.; Simaan, A. J.; Martinez, A.; Colomban, C. Bioinspired complexes confined in well-defined capsules: getting closer to metalloenzyme functionalities. *Chem. Commun.* **2023**, *59*, 4288−4299.
(40) Ikbal, A.; Colomban, C.; Zhang, D.; Delecluse, M.; Brotin, T.; Dufaud, V.; Dutasta, J.-P.; Sorokin, A. B.; Martinez, A. Bioinspired Oxidation of Methane in the Confined Spaces of Molecular Cages. *Inorg. Chem.* **2019**, *58*, 7220−7228.
(41) Kunishita, A.; Kubo, M.; Ishimaru, H.; Ogura, T.; Sugimoto, H.; Itoh, S. H_2O_2-Reactivity of Copper(II) Complexes Supported by Tris[(pyridin-2-yl)methyl]amine Ligands with 6-Phenyl Substituents. *Inorg. Chem.* **2008**, *47*, 12032−12039.
(42) Zhang, C. X.; Kaderli, S.; Costas, M.; Kim, E.-I.; Neuhold, Y.-M.; Karlin, K. D.; Zuberbühler, A. D. Copper(I)−Dioxygen Reactivity of $[(L)Cu^I]^+$ (L = Tris(2-pyridylmethyl)amine): Kinetic/Thermodynamic and Spectroscopic Studies Concerning the Formation of Cu−O_2 and Cu_2−O_2 Adducts as a Function of Solvent Medium and 4-Pyridyl Ligand Substituent Variations. *Inorg. Chem.* **2003**, *42*, 1807−1824.
(43) Dahl, E. W.; Dong, H. T.; Szymczak, N. K. Phenylamino derivatives of tris(2-pyridylmethyl)amine: hydrogen-bonded peroxodicopper complexes. *Chem. Commun.* **2018**, *54*, 892−895.
(44) Identical results were obtained using CuI(**Hm-TPA**)$^+$.
(45) The complex $Cu^I(\mathbf{L_2})(PF_6)$ was prepared (see Supporting Information and Figures S28−S31) and studied as O_2 activation catalysts under ambient light. $Cu^I(\mathbf{L_2})(PF_6)$ displays similar reactivity as the parent $Cu^I(\mathbf{L_1})^+$ complex with isolation of a major purple $Cu^{II}(\mathbf{L_2}^{PhO})(PF_6)$ product with 50% yield (Figures S32−S34) and a minor $Cu^{II}(\mathbf{L_2}^{COO})(PF_6)$ blue complex with 30% yield (Figures 4 and S27, S35 and S36).
(46) Sarangi, R. X-ray absorption near-edge spectroscopy in bioinorganic chemistry: Application to M-O_2 systems. *Coord. Chem. Rev.* **2013**, *257*, 459−472.
(47) Kau, L. S.; Spira-Solomon, D. J.; Penner-Hahn, J. E.; Hodgson, K. O.; Solomon, E. I. X-ray absorption edge determination of the oxidation state and coordination number of copper. Application to the type 3 site in Rhus vernicifera laccase and its reaction with oxygen. *J. Am. Chem. Soc.* **1987**, *109*, 6433−6442.
(48) McCann, S. D.; Stahl, S. S. Copper-Catalyzed Aerobic Oxidations of Organic Molecules: Pathways for Two-Electron Oxidation with a Four-Electron Oxidant and a One-Electron Redox-Active Catalyst. *Acc. Chem. Res.* **2015**, *48*, 1756−1766.
(49) Liu, X.-H.; Yu, H.-Y.; Huang, J.-Y.; Su, J.-H.; Xue, C.; Zhou, X.-T.; He, Y.-R.; He, Q.; Xu, D.-J.; Xiong, C.; Ji, H.-B. Biomimetic catalytic aerobic oxidation of C−sp(3)−H bonds under mild conditions using galactose oxidase model compound $Cu^{II}L$. *Chem. Sci.* **2022**, *13*, 9560−9568.
(50) Suzuki, T.; Oshita, H.; Yajima, T.; Tani, F.; Abe, H.; Shimazaki, Y. Formation of the Cu^{II}−Phenoxyl Radical by Reaction of O_2 with a Cu^{II}−Phenolate Complex via the Cu^I−Phenoxyl Radical. *Chem.-Eur. J.* **2019**, *25*, 15805−15814.
(51) Lyons, C. T.; Stack, T. D. Recent advances in phenoxyl radical complexes of salen-type ligands as mixed-valent galactose oxidase models. *Coord. Chem. Rev.* **2013**, *257*, 528−540.
(52) Thomas, F. Ten Years of a Biomimetic Approach to the Copper(II) Radical Site of Galactose Oxidase. *Eur. J. Inorg. Chem.* **2007**, *38*, 2379−2404.
(53) Connelly, N. G.; Geiger, W. E. Chemical Redox Agents for Organometallic Chemistry. *Chem. Rev.* **1996**, *96*, 877−910.
(54) In this case, stabilization of the Cu^{II}-phenoxyl radical species was only effective with the caged complex. Oxidation of $Cu^{II}(\mathbf{L_1}^{PhO})(PF_6)$ by CAN indeed resulted in the formation of insoluble precipitate, highlighting the benefits of the cage structure that prevents undesired side reactions with CAN.
(55) Any attempt to find a concerted mechanism was unsuccessful (see ESI).
(56) Hou, S.; Li, X.; Xu, J. Mechanistic Insight into the Formal [1,3]-Migration in the Thermal Claisen Rearrangement. *J. Org. Chem.* **2012**, *77*, 10856−10869.
(57) Barbieri, A.; Kasper, J. B.; Mecozzi, F.; Lanzalunga, O.; Browne, W. R. Origins of Catalyst Inhibition in the Manganese-Catalysed Oxidation of Lignin Model Compounds with H_2O_2. *ChemSusChem* **2019**, *12*, 3126−3133.

https://doi.org/10.1021/jacsau.4c00184
JACS Au 2024, 4, 1966−1974